Katarzyna Jagodzińska[1]
Faculty of Energy and Environmental Engineering,
Silesian University of Technology,
Konarskiego 20,
Gliwice K113, Poland
e-mail: kjag@kth.se

Michał Czerep
Department of Boilers, Combustion and Energy Processes,
Wroclaw University of Science and Technology,
Wybrzeże St. Wyspiańskiego 27,
Wrocław 50-370, Poland
e-mail: michal.czerep@pwr.edu.pl

Edyta Kudlek
Faculty of Energy and Environmental Engineering,
Silesian University of Technology,
Konarskiego 18,
Gliwice 44-100, Poland
e-mail: edyta.kudlek@polsl.pl

Mateusz Wnukowski
Department of Boilers, Combustion and Energy Processes,
Wroclaw University of Science and Technology,
Wybrzeże St. Wyspiańskiego 27,
Wrocław 50-370, Poland
e-mail: mateusz.wnukowski@pwr.edu.pl

Marek Pronobis
Faculty of Energy and Environmental Engineering,
Silesian University of Technology,
Konarskiego 20,
Gliwice 44-100, Poland
e-mail: marek.pronobis@polsl.pl

Weihong Yang
Department of Material Sciences and Engineering,
KTH Royal Institute of Technology,
Brinellvägen 23,
Stockholm 100 44, Sweden
e-mail: weihong@kth.se

Torrefaction of Agricultural Residues: Effect of Temperature and Residence Time on the Process Products Properties

*To date, few studies on the potential utilization of agricultural residue torrefaction products have been performed. Thus, torrefaction product characterization aimed at its potential utilization was performed. Wheat–barley straw pellets and wheat–rye chaff were used in the study. The impact of the torrefaction temperature (280–320 °C) on polycyclic aromatic hydrocarbons (PAHs) content in the biochar and noncondensable gas (noncondensables) composition was investigated. The impact of the torrefaction time (30–75 min) on the composition of the condensable volatiles (condensables) and their toxicity were also studied. The torrefaction process was performed in a batch-scale reactor. The PAH contents were measured using high-performance liquid chromatography (HPLC), and the noncondensables composition was measured online using a gas analyzer and then gas chromatograph with flame ionization detector (GC-FID). The condensables composition and main compound quantification were determined and quantified using gas chromatography–mass spectrometry (GC/MS). Three toxicity tests, for saltwater bacteria (Microtox® bioassay), freshwater crustaceans (Daphtoxkit F magna®), and vascular plants (*Lemna *sp. growth inhibition test), were performed for the condensables. The PAHs content in the biochar, regardless of the torrefaction temperature, allows them to be used in agriculture. The produced torgas shall be co-combusted with full-caloric fuel because of its low calorific value. Toxic compounds (furans and phenols) were identified in the condensable samples, and regardless of the processing time, the condensables were classified as highly toxic. Therefore, they can be used either as pesticides or as an anaerobic digestion substrate after their detoxification.* [DOI: 10.1115/1.4046275]

Keywords: biomass, polycyclic aromatic hydrocarbons, toxicity tests, energy from biomass, renewable energy

Introduction

Undeniably, worldwide energy-related industries face future challenges related to sustainable energy production and balanced energy use to address the need for action against progressive planet degradation and climate change. These challenges also occur under a circular economy that aims to be resource-efficient and to have zero-waste production systems. One of the available technologies that meet these requirements is the torrefaction of agricultural residues as they are extensively available worldwide—from wheat and barley postprocessing wastes dominant in the EU to corn and rice straw dominant in northern China [1]. Biomass is considered the most valuable renewable energy source because of its minimal dependence on climate conditions [2]. Moreover, using wastes from agricultural processing does not compete with the food production sector and, therefore, does not pose the risk of increasing the prices of crops [3].

Torrefaction has been a research subject for roughly 15 years. The term refers to thermal pretreatment in an inert atmosphere, usually at 200–300 °C. The process mainly produces fuel (biochar) with high energy density and improved grindability [4–6] as a way to mitigate the drawbacks connected with transporting, handling, and milling raw biomass. Torrefied biomass is often referred to as "biocoal" because its grindable and combustible characteristics are close to those of coal, and it is expected to replace coal in existing heat and power generation plants [7]. Given the above, biochar combustion or co-combustion has been the main subject of studies carried out to date [8–10]. Following the idea of the circular economy, however, the remaining process products have recently attracted attention as well. Moreover, an alternative application of biochar, not as fuel but as fertilizer in agriculture, has become a subject of interest [11].

Biochar is widely considered to be beneficial to the physical, chemical, and biological attributes of soil, enhancing plant growth. It has been linked to five main factors: nutrient provision, nutrient cycling intensification, changes in cation exchange

[1]Present address: KTH Royal Institute of Technology, Department of Material Sciences and Engineering, Brinellvägen 23, Stockholm, Sweden.

Contributed by the Advanced Energy Systems Division of ASME for publication in the Journal of Energy Resources Technology. Manuscript received July 9, 2019; final manuscript received January 6, 2020; published online February 10, 2020. Assoc. Editor: Ashwani K. Gupta.

capacity, positive changes in soil pH, and, finally, an increase in the dynamics of water in the soil. Additionally, biochar adsorbs hydrophobic organic pollutants in the soil [12,13]. However, the process of biochar production (torrefaction) is accompanied by the formation of polycyclic aromatic hydrocarbons (PAHs) as a result of Diel–Alder reaction occurring during the process [14]. These hydrocarbons are considered to be toxic, and for this reason, their emissions to the environment are legally limited and strictly monitored. Thus, the PAHs content in biochar must be examined when considering the soil application of biochar. Unfortunately, the available literature does not offer a tool for predicting PAHs content in biochar, as the data do not show an overall trend in the relationship between PAHs formation and process parameters. PAHs content is strongly related to the feedstock type and process temperature [15], but a consensus has not yet been reached on this relationship [16]. Therefore, the authors investigated the PAHs content in biochar torrefied at different temperatures to evaluate its possibility of being used as fertilizer.

Another product of torrefaction is a gas (torgas) that is released during the process. These volatiles are a mixture of condensable (condensables) and noncondensable compounds. In most pilot-scale installations, torgas is used as a source of heat within the process [17–19], making its quality essential from a practical point of view [20]. In that case, condensable compounds are incinerated as a part of torgas. The proper insulation of gas feed lines is crucial to avoid condensation, which may cause operational problems [21,22] because condensed compounds can be highly corrosive to combustion equipment and can clog gas ducts. In this study, the condensables were removed from the torgas (condensed), and the composition and calorific value (CV) of the noncondensable compounds at different torrefaction temperatures were investigated.

The condensables removed from the torgas were also analyzed in the study. The composition of the condensables from wheat straw torrefaction has been extensively studied in the past [23,24], but only a few studies on condensables utilization can be found in the available literature. These studies mainly concern condensables from woody biomass torrefaction and their applications as biodegradable pesticides [25], wood protection agents [26], or anaerobic digestion substrates [27]. The method of condensables utilization differs for different feedstocks as well as for different process parameters. As the majority of previous studies focus on woody biomass, the authors of this study addressed this gap by investigating the relationship between the composition and toxicity of the condensables from agricultural residues torrefaction and the duration of the process to preliminarily assess their potential for further application. The impact of the process temperature on the possibility of using torrefaction condensables as anaerobic digestion substrates has been investigated in a previous paper [28].

Given the above, the main objective of the study was to preliminarily assess the potential of torrefaction products for further application. The impact of process temperature on PAHs content in biochar produced at different torrefaction temperatures was investigated to determine the possibility of its utilization as fertilizer. The impact of process duration on condensables composition and their toxicity was investigated to determine the possible mechanism of their utilization. Additionally, the impact of torrefaction temperature on noncondensables composition and the calorific value was studied because noncondensables are a great potential source of heat necessary for the torrefaction process. The feedstocks used in the study were agricultural residues in the form of wheat–barley straw pellets and wheat–rye chaff as they are the most common agricultural wastes in central Europe (Germany and Poland).

Materials and Methods

Feedstock Properties. The study was performed for two types of feedstock: wheat–barley straw pellets and wheat–rye chaff.

Wheat–barley straw pellets, referred to as WB, are commercially used in Germany. The wheat–barley volume ratio is 95/5, and the dimensions of the pellets are as follows: $\phi = 15$ mm and length = 29–30 mm. There was no binding agent used during pelletization [28].

Wheat–rye chaff, referred to as WR, is a common agricultural waste in Poland. The average length of the stalks is 30 mm.

Table 1 The results of the elemental and proximate analysis of the feedstocks [28]

Parameter/Symbol/Unit			WB		WR	
Ash content	A^a	%	10.76	±0.38	6.48	±0.23
Sulfur content	S^a	%	0.13	±0.01	0.09	±0.00
Carbon content	C^a	%	44.14	±1.28	45.94	±1.32
Hydrogen content	H^a	%	5.49	±0.25	5.82	±0.26
Nitrogen content	N^a	%	0.86	±0.05	0.57	±0.03
Chlorine content	Cl^a	%	0.43	±0.075	0.188	±0.033
Sodium content	Na^a	%	0.08	±0.01	0.02	±0.01
Potassium content	K^a	%	1.43	±0.20	0.89	±0.13
Oxygen content[b]	O^a	%	38.19	±0.26	40.91	±0.26
Mercury content	Hg^a	mg/kg	0.018	±0.003	0.013	±0.002
Lower heating value	LHV^a	MJ/kg	16.27	±0.63	17.35	±0.67
Volatile matter content	V^c	%	77.20	±1.49	77.69	±2.40

[a]Dry state.
[b]Calculated as 100%—sum of other element contents.
[c]Dry ash-free.

Table 1 shows the results of the elemental and proximate analysis of the feedstocks [28]. WR is characterized by a lower ash content than that of WB, which results in a slightly higher lower heating value. Notwithstanding this factor, no significant differences in elemental composition exist; therefore, feedstocks can be considered similar.

An external lab (Zakłady Pomiarowo-Badawcze Energetyki "ENERGOPOMIAR" Sp. z o. o., Gliwice, Poland) analyzed the feedstocks according to: EN 15407:2011 using infrared and thermal conductivity detection (C, H, N, and S contents), EN 15408:2011 using ion chromatography (Cl content), EN ISO 18125:2017-07 (lower heating value), and EPA method 7473:2007 (Hg content). Na and K contents were determined using inductively coupled plasma-optical emission spectrometry following an internal procedure of an external laboratory.

The authors determined the volatile matter content in a dry ash-free state (V^{daf}) content according to ISO 18123:2015.

Torrefaction Process. As stated before, the study was performed on two types of agricultural residues, which are similar in terms of their chemical compositions: wheat–rye chaff (WR) and wheat–barley straw pellets (WB). The change in the feedstock was directly connected to its form—in comparison to WB, the chaff form resulted in better control over uniformly heating the material of the whole volume over the particular time. For that reason, WR was used as the feedstock for the study of condensable composition and toxicity with respect to the process duration.

The masses of the WR and WB samples were 1 kg and 2 kg, respectively, which corresponded to approximately half-filling of the torrefaction reactor.

The study was preceded by TG analysis and a set of trial tests, which allowed the selection of the temperature range and the duration of the process.

WB was torrefied within the temperature range of 240–320 °C with a step of 20 °C. The holding time at the final temperature was 75 min—a significant decrease in torgas yield indicated the end of the process.

WR was torrefied at 280 °C and its holding times at that temperature were 30 min, 60 min, and 75 min.

Figure 1 shows the main stages of the study.

The torrefaction process was performed in a laboratory-scale batch reactor, shown in Fig. 2 [28]. The reactor was heated by the heating mantle that consisted of three ceramic-insulated band

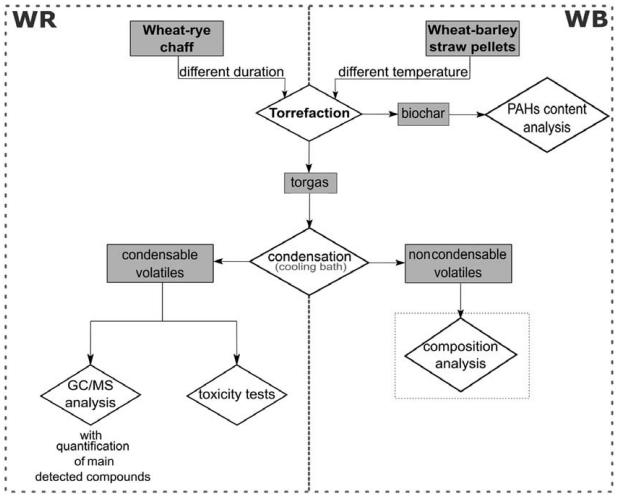

Fig. 1 Flowchart presenting the main stages of the study

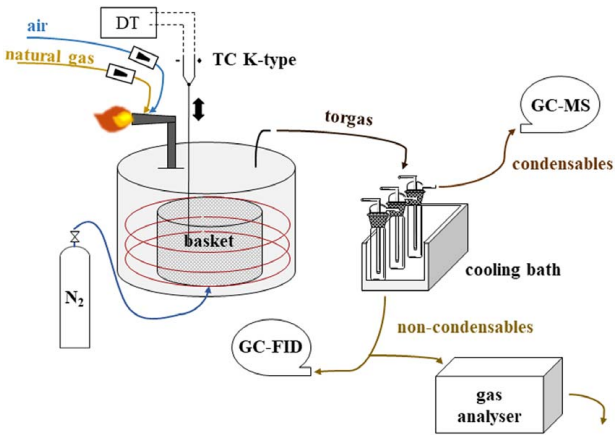

Fig. 2 A general scheme of the test rig (DT, digital thermometer; TC, thermocouple; and GC-FID, gas chromatograph with flame ionization detector) [28]

heaters, regulated by a programmable logic controller connected with a type K thermocouple in one of the bands. A random order of experiments was introduced to avoid consecutive run errors.

The sample was introduced into the reactor in a stainless-steel mesh basket of the following dimensions: $\phi = 300$ mm; height = 450 mm; and aperture = 0.5 mm, and then, the reactor was closed. During heating, the sample was manually mixed by a two-bladed centrifugal stirrer. A K-type thermocouple, immersed in the sample, was used to measure the temperature. As immersion of the thermocouple was regulated, the temperature of the sample was measured every 5 min along its thickness.

From the moment the reactor closed, the noncondensables composition was measured. Until the O_2 content in the gas was lower than 3 vol%, the reactor was flushed with nitrogen to purge the air from the setup, which was only during the initial stage of heating, for ~20 min. Then, the amount of torgas produced in the reactor was enough to prevent air leaching into the reactor.

Torgas spewed out through two stub pipes—one directly connected with the flare on the top of the reactor and the second connected with the sampling path. The flare was supplied with air and natural gas to stabilize the flame. The sampling path consisted of a condensing section (a set of impingers immersed in a cooling bath with propylene glycol at 0.5 °C), a conditioner, and a gas analyzer. Trial tests showed that most of the condensable volatiles were a group of polar compounds, and for that reason, deionized water was chosen as a solvent in the impingers. Two impingers, each with 100 cm^3 of solvent, were used as they allowed sufficient capture of volatiles, which was consistent with the findings of Bergman et al. [29] and Tumuluru et al. [30].

After each experiment, impinger contents (condensables) were mixed, stirred, and heated to the ambient temperature. In the case of wheat–barley straw pellets, each condensable solution was filtered to separate water-soluble and water-insoluble (liquid gel) compounds. Wheat–rye chaff torrefaction did not result in the formation of liquid gel.

The volume rate of the torgas was not measured. For this reason, the mass balance closure was performed by calculating the gas yield as the difference between 100% and the sum of the other product yields.

Torrefaction Products Characterization

Polycyclic Aromatic Hydrocarbons Content in Biochar. At the end of each test, the biochar was collected and weighed. Then, the samples were ground in a knife mill (LMN-240; TESTCHEM, Radlin, Poland) with a maximum capacity of 90 kg/h, with 5 mm, 2 mm, and 1 mm sieves, and then, respective samples were formed by quartering.

The contents of the 15 PAHs (without acenaphthylene) in the torrefied wheat–barley straw pellets were analyzed by an external laboratory (Zakłady Pomiarowo—Badawcze Energetyki "ENERGOPOMIAR" Sp. z o.o., Gliwice, Poland). The contents were measured using high-performance liquid chromatography (HPLC) according to the ISO 13877:2004 standard.

Noncondensables Property Characterizations. An online analysis of the noncondensables composition was performed using the Gas 3100R analyzer (supplied by Atut Sp. Z O.O. Lublin, Poland). The analyzed compounds, type of detectors used, and the maximum measuring ranges are shown in Table 2. The accuracy of the measurement was 1% of the measuring range. The gas analyzer was calibrated before each test using nitrogen (purity of 5.0).

The gas samples were also collected in gas bags and further analyzed using an Agilent HP 6890 gas chromatograph with flame ionization detector (GC-FID). The samples were introduced through the sampling loop into the GC injector (200 °C; split = 5); helium was used as carrier gas (55 kPa). The GC was equipped with RT-Alumina Bond/KCl column (50 m × 0.53 mm × 10 μm; Restek), and the temperature profile (for qualitative analysis) was as follows: holding at 45 °C for 1 min, then increasing with 10 K/min to 200 °C and holding for 5 min. The quantification, based on calibration curves, was performed using methane calibration standards (Linde Gas); the temperature profile involved holding at 100 °C for 10 min.

Condensables Property Characterization. Condensables from the wheat–rye chaff were subjected to GC/MS analysis (Agilent 7820 gas chromatography coupled with an Agilent 5977B MSD mass spectrometer) using a Stabilwax-DA column (30 m × 0.32 mm × 0.25 μm; Restek). The analysis procedure was the same as that reported in Ref. [28]. The MS scanning range was m/z 10–450 with a frequency of 1.7 scans/s. The gain factor and EM volts were 0.5 and 1348.5, respectively, and the MS source

Table 2 The analyzed noncondensable compounds, type of detector used, and the maximum measuring ranges for each compound

Analyzed compound	Detector	Max. measuring range, %
C_xH_y—a sum of ethane, propane, and butane	NDIR sensor	5
CH_4	NDIR sensor	10
CO	NDIR sensor	40
CO_2	NDIR sensor	100
H_2	TCD	55
O_2	ECD	25

and quadrupole temperatures were 230 °C and 150 °C, respectively. Samples (0.5 μl) were manually introduced to the GC injector at 250 °C (split = 20) with helium as the carrier gas (1.5 ml/min). The temperature profile was as follows: holding at 50 °C for 5 min, heating with 10 K/min to 200 °C, and holding for 20 min. The identification of the compounds was conducted automatically with the minimum match factor with the NIST-14 library of 80%. The results of the GC/MS analysis are presented in the form of weight-normalized area% to enable comparison of the samples and identification of trends. The weigh-normalization was performed by multiplying the area% by the weight yield of the condensables from each experiment.

A part of the major compounds was quantified according to the external standard method [31]. The quantification was extended with pyridine, pyridin-3-ol, and acetamide, which were not detected during the GC/MS qualitative analysis. The calibration curves were determined by creating four points of known compound concentrations in an isopropanol-compound solution. Each point was verified five times to ensure the repeatability of the results. The isopropanol and quantified compounds shown later in the Results section were of a chromatographic grade (Sigma Aldrich and Chempur, Poland for phenol).

The condensables from the wheat–rye chaff were subjected to three acute toxicity tests: the Daphtoxkit F magna® survival bioassay, the Microtox® bioassay, and the *Lemna* sp. growth inhibition test. These tests were performed to assess the environmental impact of the condensables on different trophic levels and thus initially determine their potential application.

The tests were first performed for the undiluted sample of the condensables and then for the diluted samples with deionized water until measurable results were obtained. The dilution of 1:1000 was the first one that provided quantifiable results that are noted in this paper.

The survival bioassay Daphtoxkit F magna® (Tigret, Warsaw, Poland) was performed following the OECD Guideline 202, ISO 6341, and ASTM E1440-91 standards. The test times (the time after which the number of dead organisms was evaluated) were 24 h and 48 h.

The enzymatic Microtox® bioassay was performed following the screening test procedure of the MicrotoxOmni system in the Microtox Model 500 analyzer (Modern Water, Warsaw, Poland) with exposure times of 5 min and 15 min. In this test, *Aliivibrio fisheri* are the indicator organisms for which bioluminescence is measured during the test, in reference to a 2% NaCl solution as a control sample; the change in their bioluminescence is related to the inhibition of their metabolic processes. The pH of the analyzed samples met the requirements of the manufactured analyzer (pH in the range of 6.0–8.5); therefore, no pH corrections were performed.

The *Lemna* sp. growth inhibition test was performed following the OECD Guideline 221 for the plant from own breeding. The test was conducted at 25 ± 1 °C, and the light illuminance was 6000 lux. The test results were compared with those of the control sample.

Results and Discussion

Impact of the Torrefaction Temperature and Time on the Product Yields. Figure 3 shows the torrefaction product yields for the wheat–barley pellets [28] and wheat–rye chaff. They are calculated in reference to the initial feedstock mass in a dry ash-free state. The exact values of the yields are shown in Table S1 available in the Supplemental Materials on the ASME Digital Collection. The condensables were divided into water-soluble compounds and liquid gel. Wheat–barley straw pellets were torrefied for 75 min at different temperatures, whereas the wheat–rye chaff was torrefied at 280 °C for 30 min, 60 min, and 75 min.

With the temperature increase from 240 °C to 260 °C, the biochar and condensable yields increased, whereas with a further temperature increase, the change was slight. The slight change was caused by cracking and secondary reactions of condensable volatiles, which resulted in the formation of compounds characterized

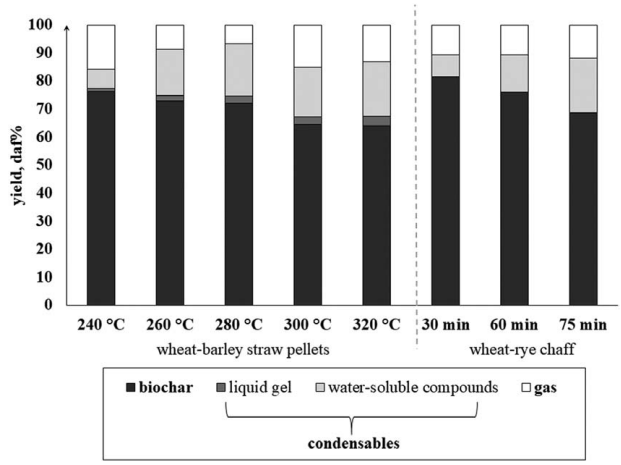

Fig. 3 Torrefaction product yields calculated in reference to the initial feedstock mass in a dry ash-free state

by lower molecular weights, some of which became part of noncondensables [28,32]. With the temperature increase, a liquid gel yield increase was observed as well, which was a result of nonpolar or slightly polar compound formation (such as benzene derivatives). In general, with the torrefaction temperature increase, the biochar yield decreased in favor of condensables and noncondensables yields, which is consistent with data in the literature [19,33].

With the torrefaction time increase, the yield of biochar decreased in favor of the condensables and noncondensables yield. This result is also consistent with the available data in the literature. For the WR, no liquid gel was formed, which also was reflected in the GC/MS analysis, where no aromatics, esters, or other nonpolar compounds were detected.

Impact of the Torrefaction Temperature on the Polycyclic Aromatic Hydrocarbons Content in the Biochar. During the torrefaction of biomass, organic compounds are partially cracked in unstable fragments, composed of highly reactive free radicals, which then react with surrounding compounds and form more stable PAHs [12]. They are formed directly via lignin, cellulose, and hemicellulose dehydrogenation, dealkylation and aromatization; the elimination of functionalities in the compounds such as H_2O, CO_2, CH_4, and H_2S, results in aromatized structures [16].

Table 3 shows the contents of 15 PAHs, determined for two samples—wheat–barley straw pellets torrefied at 320 °C and

Table 3 PAH content in two wheat–barley pellet samples torrefied at 280 °C (WB_280) and 320 °C (WB_320)

	Content, mg/kg	
PAH	WB_280	WB_320
Naphthalene	<0.01	<0.01
Acenaphthene	0.54 ± 0.12	<0.01
Fluorene	0.03 ± 0.01	<0.01
Phenanthrene	0.012 ± 0.004	5.01 ± 1.5
Anthracene	<0.01	0.17 ± 0.02
Chrysene	<0.01	<0.01
Fluoranthene	0.03 ± 0.01	4.59 ± 1.24
Pyrene	<0.01	<0.01
Benz[a]anthracene	<0.01	<0.01
Benzo[b]fluoranthene	<0.01	<0.01
Benzo[k]fluoranthene	<0.01	<0.01
Benz[a]pyrene	<0.01	<0.01
Dibenz[a,h]anthracene	<0.01	<0.01
Benzo[g,h,i]perylene	<0.01	<0.01
Indeno[1,2,3-c,d]pyrene	<0.01	<0.01
SUM:	~0.61 ± 0.14	~9.77 ± 2.76

280 °C. The samples torrefied at lower temperatures (240 °C and 260 °C) are not shown due to the PAHs concentrations being under the detection limits.

Acenaphthene, fluorene, phenanthrene, anthracene, and fluoranthene were detected in the analyzed samples. At lower temperatures (280 °C), acenaphthene dominated, followed by fluorene and fluoranthene. At higher temperatures (320 °C), acenaphthene and fluorene were not detected due to their boiling points of <300 °C; in contrast, heavier compounds than acenaphthene and fluorene were formed, including four-ring fluoranthene.

The high concentration of PAHs and the formation of more ringed species with the temperature increase were consistent with the results of Keiluweit et al. [15]. On the other hand, Freddo et al. [13] showed higher PAHs concentrations in rice straw pyrolyzed at 300 °C than those at 600 °C.

Devi and Saroha [34] analyzed PAHs concentrations in biochar from paper mill effluent treatment plant sludge pyrolysis in the temperature range of 200–700 °C, which resulted in a significant increase in naphthalene, acenaphthene, fluorene, phenanthrene, and fluoranthene between 200 and 300 °C and a decrease in anthracene and pyrene. Thus, hemicellulose and cellulose decomposition led to the formation of relatively heavy molecules at low temperatures and an increase in PAHs content with increasing temperature. The reverse trend was reported by Wang et al. [16], where relatively light PAHs were formed at low temperatures, whereas relatively heavy PAHs were formed at high temperatures. The diversification of the research results led researchers to the conclusion that temperature alone is not the main factor influencing PAHs formation [14,15,35]—their formation seems to be a result of the synergic influence of temperature and feedstock type.

Furthermore, some of the previous studies showed that lignin decomposition resulted in an increase in PAHs concentration [16]. Lignin degrades at temperatures in the range of 180–300 °C [36] and is considered to be decomposed to a large extent at temperatures higher than 300 °C [37]. Our results show that at 320 °C, the number of PAHs in the WB biochar increased significantly with the tendency to form heavier molecules, which may suggest that the large lignin decomposition results in additionally enhanced PAHs formation.

According to the European Biochar Certificate Guidelines for a Sustainable Production of Biochar [38], the sum of 16 PAHs for premium-grade biochar must be lower than 4 mg/kg, whereas the limit for the basic-grade biochar is 12 mg/kg. All of the analyzed biochar samples met the requirement for basic-grade biochar, whereas those from lower temperatures (240 °C, 260 °C and 280 °C) can be considered premium-grade biochar. Therefore, they could be used in agriculture as fertilizers.

The Impact of the Torrefaction Temperature on the Torgas Composition. Figure 4 shows the average noncondensables composition and the calorific value at different torrefaction temperatures. The exact values are shown in Table S2 available in the Supplemental Materials on the ASME Digital Collection. The measuring error does not exceed 1 percentage point (pp) for CO_2, 0.4 pp for CO, 0.25 pp for O_2, 0.1 pp for CH_4, and 0.05 pp for C_nH_m. Unmeasured components are marked as "others."

The CO_2 and CO contents slightly increased with increasing temperature as a result of hemicellulose and cellulose decomposition, whereas the CH_4 content decreased with increasing temperature. The CO_2 and CO trends were consistent with that in the available literature [39], whereas the CH_4 trend was not consistent. Chen et al. [40] analyzed rice husk torrefaction products obtained at 210 °C, 240 °C, 270 °C, and 300 °C, and the formation of CH_4 began at 270 °C. The amount of CH_4 increased at 300 °C, whereas Nam and Capareda [41] detected the start of CH_4 formation at 250 °C with an increasing trend in temperature as well. Both Chen et al. [40] and Nam and Capareda [41] used feedstocks with similar cellulose, hemicellulose, and lignin contents to analyzed wheat–barley straw pellets; therefore, it is likely that the process

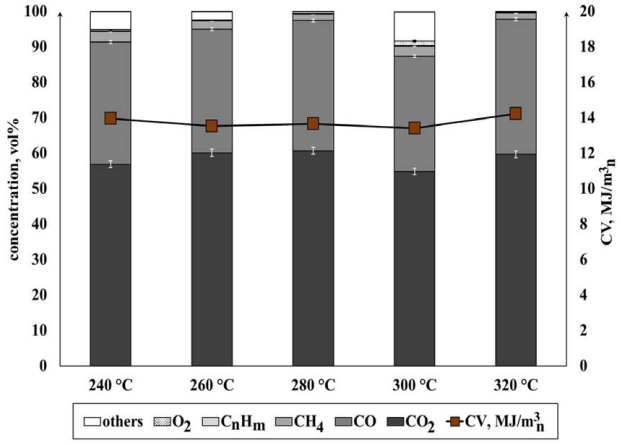

Fig. 4 Average compositions of noncondensables from the wheat–barley pellet (CV, calorific value)

conditions (i.e., feedstock heating rate) impacted the methane formation profile with temperature, which was the reason for the discrepancy between the obtained results and the available data in the literature.

CO_2 and CO are formed as a result of decarboxylation and depolymerization reactions (breakage of C—O—C and C═O bonds in hemicellulose, cellulose, and aldehydic compounds as a result of their secondary pyrolysis reaction), whereas CH_4 is a result of depolymerization and cracking [32]. According to Chen et al. [42], deoxidation of hemicellulose plays a major role in oxygen release, and during this process, the amount of O_2 released as volatiles (H_2O, CO, CO_2, and oxygen-containing organic compounds) significantly increases. The decomposition of cellulose is relatively slow and results mainly in CO_2 and CO, whereas the decomposition of lignin results in oxygen transforms mainly to H_2O. Moreover, during lignin decomposition, small amounts of CH_4 and H_2 can be measured due to the alkyl branches and methoxyl functional groups in its structure.

At 300 °C, CO_2 and CO contents slightly decreased in favor of CH_4, C_nH_m and "other" compounds. It is likely that "other compounds" were higher hydrocarbons. Moreover, a slight amount of H_2 was detected at this temperature. The detection of H_2 combined with an increase in O_2 and an increase in CH_4 and C_nH_m contents may suggest the beginning of lignin decomposition. Then, at 320 °C, the main parts of the carbon and oxygen from lignin were transferred to the form of condensable compounds, and the torgas parameters were similar to those at 280 °C.

The average CV of the gas was 13.71 MJ/m^3_n, and there was no significant difference in the CV between the samples. This relatively low calorific value demonstrated that co-combustion with full-caloric fuel was the most favorable utilization mechanism. This fuel can be either natural gas [19] or part of dried or already torrefied biomass [22] and will depend on determining the economic feasibility of those solutions through additional research.

Figure 5 shows the yield of different C_nH_m components (determined with GC-FID) of the chosen noncondensable samples. The exact concentrations of the gases are shown in Table S3 available in the Supplemental Materials on the ASME Digital Collection. The measurement error does not exceed 2.9 pp. There was no difference in the light hydrocarbons content between the samples at 300 °C and 320 °C, whereas the sample at 260 °C was characterized by a higher content of lighter hydrocarbons than that of the other samples. This result shows a tendency to form higher molecules at higher temperatures.

The Impact of the Torrefaction Time on the Condensables Composition. The impact of the torrefaction time on the condensable volatiles (condensables) composition was investigated for the

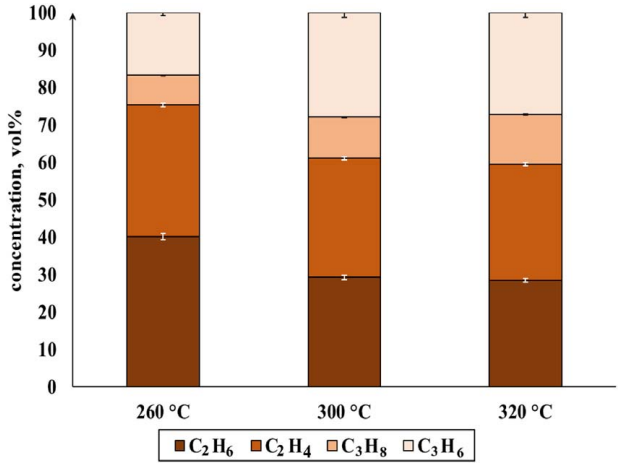

Fig. 5 The results of the GC-FID analysis of C_nH_m in the noncondensables

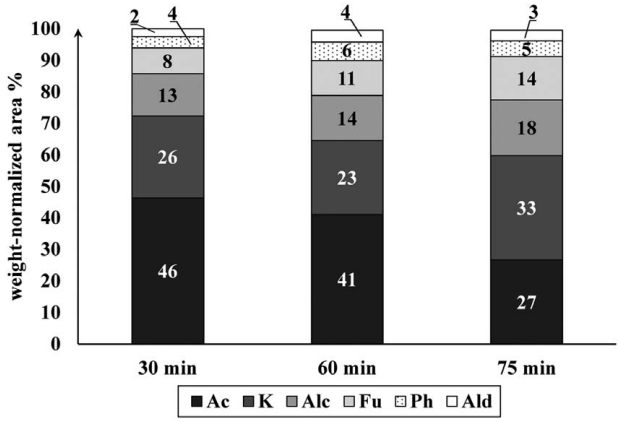

Fig. 6 Composition of the condensables from wheat–rye chaff torrefaction (Ac, acids; K, ketones; Alc, alcohols; Fu, furans; Ph, phenols; Ald, aldehydes)

wheat–rye chaff. The torrefaction times were 30 min, 60 min, and 75 min, and the process temperature was 280 °C. The list of detected compounds can be found in Tables S4 and S5 available in the Supplemental Materials on the ASME Digital Collection.

The detected compounds were divided into six main groups, as shown in Table S6 available in the Supplemental Materials on the ASME Digital Collection. Figure 6 shows the weight-normalized peak area distribution of those groups in the condensables. Esters (e.g., methyl 2-hydroxy-2-methylbutanoate) and unknown compounds (not identified because of missing spectral or chromatographic data) were also detected in the samples. Their area%, however, was slight (in the range of 0–0.4), and therefore, they are not shown in Fig. 6.

The number of detected compounds increased with increasing torrefaction time. The compounds were consistent with those detected in previous studies [23,43], as the thermal decomposition of biomass (hemicellulose, cellulose, and lignin) results in the formation of anhydrosugars, phenols, and pyrans, which then decompose to lighter compounds such as ketones or acids. This decomposition is caused by secondary reactions, inter alia side-chain splitting or ring scission [44].

The acid group dominated in the analyzed samples, although with increasing torrefaction time, their amount decreased in favor of ketones and alcohols. Acetic acid was the main compound, which corresponded to 20–40 pp of the whole weight-normalized area%.

Acetic acid and methanol have been identified (quantified) as the main components in torrefaction condensates from lignocellulosic biomass [45–47], which is consistent with the quantification results of this study. Figure 7 shows the results of the quantitative analysis of acetic acid content with torrefaction duration; its content increased until the final stage of torrefaction (after 60 min), when it was transformed into other compounds as a result of secondary reactions. In parallel, acetamide, derived from acetic acid, showed the same tendency (Fig. 8). On the other hand, the butanoic acid concentration increased with the increase in torrefaction duration (Fig. 8) as well as methanol concentration (Fig. 7).

With increasing time, the number of aldehydes and ketones that formed increased (Fig. 6). This result was related to the additional C and O from hemicellulose that was transferred to the condensables [41]. Among the ketone group, 1-hydroxypropan-2-one (hydroxyacetone) was dominant as a result of secondary reactions of propan-2-one derived from hexose-containing polysaccharides such as β-glucan [48]. Acetaldehyde was the main aldehyde detected in the samples, which was consistent with the results of Commandre and Leboeuf [47] for wheat straw torrefaction.

Furan-2-carbaldehyde (furfural) is the main compound in the furan group (Fig. 6), followed by 1-(furan-2-yl)ethenone (acetylfuran) and then furan-2-ylmethanol (furfuryl alcohol). Furfural production is a result of hemicellulose decomposition [49], whereas acetylfuran and furfuryl alcohol formation is the result of secondary reactions, such as hydrolysis and acylation of furans; the longer the torrefaction duration is, the higher their content.

The yield of phenolics was stable in the analyzed samples (Fig. 6). All condensables were obtained at 280 °C, which was below

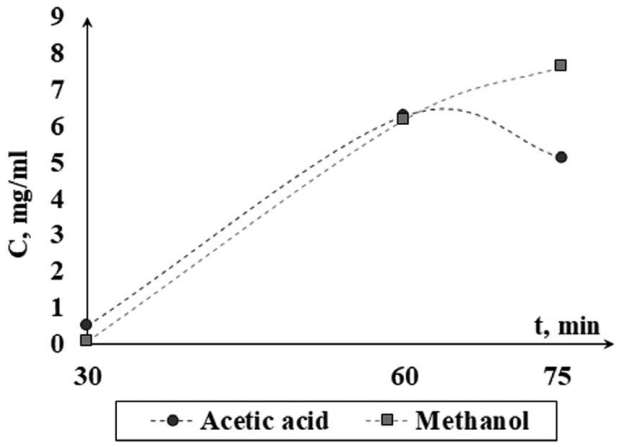

Fig. 7 The results of the quantitative analysis of acetic acid and methanol contents in the condensables from wheat–rye chaff torrefaction (the measurement errors do not exceed 3.13%)

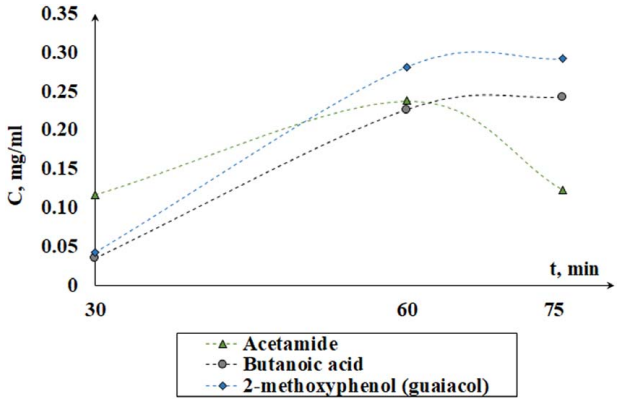

Fig. 8 The results of the quantitative analysis of acetamide, butanoic acid, and guaiacol contents in the condensables from wheat–rye chaff torrefaction (the measurement errors do not exceed 1.45%)

the temperature at which lignin was decomposed in large part. Therefore, the phenolic content was mainly connected to the progressive decomposition of hemicellulose; for example, guaiacol formation is the result of arabinoxylan decomposition linked to ferulic acid (lignin-like compound) [48].

Figures 8 and 9 show the changes in the phenol group composition. 2-methoxy-4-vinylphenol (guaiacol) was detected as one of the main phenolics, which is consistent with the results of Lê Thành et al. [24]; its concentration increased with increasing process time. The same scenario was observed for guaiacol-derived compounds (4-ethyl-2-methoxyphenol and 4-ethenyl-2-methoxyphenol)—the longer the process time, the higher their concentration. The guaiacol derivatives were formed during the secondary reactions of guaiacol, similar to the previously mentioned furfural derivatives formed in the secondary reactions of furfural.

A small amount of pyridines (pyridine and pyridin-3-ol) was also detected (Fig. 9). Their content increased until the final phase of the process, during which they were decomposed.

The exact values of the quantified compound concentrations are shown in Table S7 available in the Supplemental Materials on the ASME Digital Collection.

The Impact of the Torrefaction Time on the Condensables Toxicity. Three bioassays were performed for the condensable volatiles (condensables) from the wheat–rye chaff torrefaction—the enzymatic Microtox® bioassay, the survival bioassay Daphtoxkit F magna®, and the *Lemna* sp. growth inhibition test. These tests were performed in condensable-deionized water solutions with a 1:1000 dilution ratio.

The samples were classified according to a commonly used method [50], which includes two classes of acute toxicity; a toxicological effect in the range of 50.1–75% means that the solution is toxic, and when it is in the range of 75.1–100%, the solution is considered to be highly toxic. For this reason, 75.1% was marked as a limit in Fig. 10.

The *Lemna* sp. growth inhibition test resulted in a toxicological effect equal to 100% as the analyzed condensables caused inhibition of plant growth and then necrosis. This result means that the introduction of these samples into the environment, in an unchanged state, will have an adverse effect on vascular plants. Therefore, the results of these tests are not shown in Fig. 10.

Figure 10 shows the Microtox® bioassay (exposure time: 5 min and 15 min) and Daphtoxkit F magna® bioassay (exposure time: 24 h and 48 h) results for the analyzed samples. The measurement error did not exceed 5%. The results of the performed tests correlate with each other; the longer the exposure time was, the higher the toxicological effect. In all the cases, the limit level of the toxicology effect was exceeded, and therefore, all the samples were classified

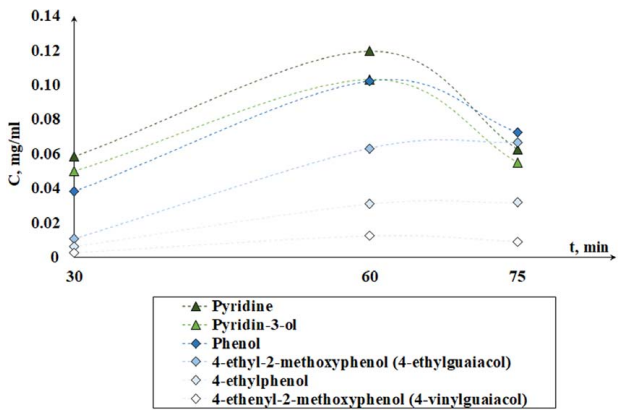

Fig. 9 The results of the quantitative analysis of some of the pyridine and phenolic contents in the condensables from wheat–rye chaff torrefaction (the measurement errors do not exceed 2.5%)

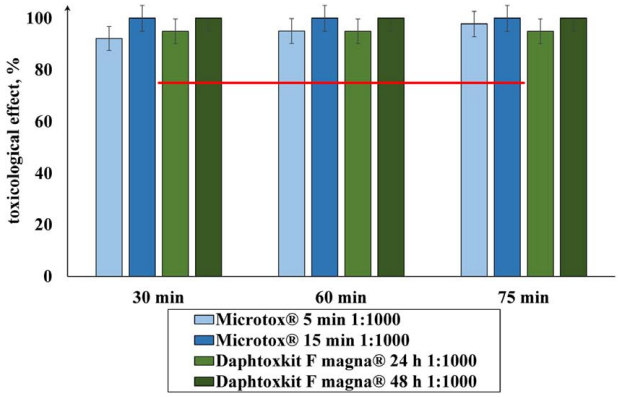

Fig. 10 The results of the toxicity tests with the limit, marked in red, above which samples are highly toxic (legend: the test name, the test time, and the sample dilution ratio)

as highly toxic, regardless of the exposure time and the torrefaction time.

The condensables from the wheat–rye chaff torrefaction contained many compounds (e.g., furans and phenolics), which are inhibitors to microbes [51,52], and many of these compounds are generally considered toxic to the environment. This result was confirmed by the results of the performed toxicity tests. Thus, the direct introduction of condensables into the environment constitutes a great risk. Therefore, Doddapaneni et al. [53] proposed a biomass torrefaction system with the detoxification of condensables using biochar and subsequently used detoxicated condensables as anaerobic digestion substrates. This approach may be one mechanism for condensable utilization. Another mechanism that will be considered and further investigated is their utilization as pesticides.

Conclusions

A study on the torrefaction temperature effect on PAHs content in the biochar and torgas composition was performed. Additionally, the impact of the torrefaction time on condensable volatiles (condensables) composition and toxicity was determined. The analysis was aimed at the preliminary assessment of the potential utilization of torrefaction products.

The main conclusions from the study can be summarized as follows:

(1) The higher the torrefaction temperature was, the higher the PAHs content in the biochar. Analyzed wheat–barley straw pellets torrefied at 320 °C met the requirement for basic grade biochar according to European Biochar Certificate classification. The samples torrefied at lower temperatures can be considered as a premium-grade biochar. This result means that all the analyzed samples could be used in agriculture.
(2) The torrefaction temperature slightly impacted the torgas composition and its calorific value. Due to its low calorific value, co-combustion with full-calorific fuel should be considered in further studies.
(3) The longer the torrefaction process was, the more heterogeneous the condensable composition because more intensive secondary reactions of the condensable volatiles occurred, which resulted in the transformation of basic compounds, e.g., the formation of guaiacol and furfural derivatives.
(4) Regardless of the process duration, condensables shall be considered highly toxic to the environment. For this reason, the utilization of condensables should involve either their prior detoxification and use, for example, as an anaerobic digestion substrate, or use directly as pesticides.

References

[1] Meng, X., Zhou, W., Rokni, E., Zhao, H., Sun, R., and Levendis, Y. A., 2019, "Effects of Air Flowrate on the Combustion and Emissions of Blended Corn Straw and Pinewood Wastes," ASME J. Energy Resour. Technol., **141**(4), p. 042205.

[2] Lenis, Y. A., Maag, G., De Oliveira, C. E. L., Corredor, L., and Sanjuan, M., 2019, "Effect of Heat Flux Distribution Profile on Hydrogen Concentration in an Allothermal Downdraft Biomass Gasification Process: Modeling Study," ASME J. Energy Resour. Technol., **141**(3), p. 031801.

[3] Haykiri-Acma, H., and Yaman, S., 2019, "Effects of Dilute Phosphoric Acid Treatment on Structure and Burning Characteristics of Lignocellulosic Biomass," ASME J. Energy Resour. Technol., **141**(8), p. 082203.

[4] Xue, J., and Goldfarb, J. L., 2018, "Enhanced Devolatilization During Torrefaction of Blended Biomass Streams Results in Additive Heating Values and Synergistic Oxidation Behavior of Solid Fuels," Energy, **152**, pp. 1–12.

[5] Poudel, J., Karki, S., and Oh, S. C., 2018, "Valorization of Waste Wood as a Solid Fuel by Torrefaction," Energies, **11**(7), pp. 1–10.

[6] Rokni, E., Liu, Y., Ren, X., and Levendis, Y. A., 2019, "Nitrogen-Bearing Emissions From Burning Corn Straw in a Fixed-Bed Reactor: Effects of Fuel Moisture, Torrefaction, and Air Flowrate," ASME J. Energy Resour. Technol., **141**(8), p. 082202.

[7] Dhungana, A., Basu, P., and Dutta, A., 2012, "Effects of Reactor Design on the Torrefaction of Biomass," ASME J. Energy Resour. Technol., **134**(4), p. 041801.

[8] Howell, A., Beagle, E., and Belmont, E., 2018, "Torrefaction of Healthy and Beetle Kill Pine and Co-Combustion With Sub-Bituminous Coal," ASME J. Energy Resour. Technol., **140**(4), p. 042002.

[9] Ren, X., Meng, X., Panahi, A., Rokni, E., Sun, R., and Levendis, Y. A., 2018, "Hydrogen Chloride Release From Combustion of Corn Straw in a Fixed Bed," ASME J. Energy Resour. Technol., **140**(5), p. 051801.

[10] Sarikaya, A. C., Acma, H. H., and Yaman, S., 2018, "Synergistic Interactions During Cocombustion of Lignite, Biomass, and Their Chars," ASME J. Energy Resour. Technol., **141**(12), p. 122203.

[11] Glaser, B., Wiedner, K., Seelig, S., Schmidt, H. P., and Gerber, H., 2015, "Biochar Organic Fertilizers From Natural Resources as Substitute for Mineral Fertilizers," Agron. Sustain. Dev., **35**(2), pp. 667–678.

[12] Hale, S. E., Lehmann, J., Rutherford, D., Zimmerman, A. R., Bachmann, R. T., Shitumbanuma, V., O'Toole, A., Sundqvist, K. L., Arp, H. P. H., and Cornelissen, G., 2012, "Quantifying the Total and Bioavailable Polycyclic Aromatic Hydrocarbons and Dioxins in Biochars," Environ. Sci. Technol., **46**(5), pp. 2830–2838.

[13] Freddo, A., Cai, C., and Reid, B. J., 2012, "Environmental Contextualisation of Potential Toxic Elements and Polycyclic Romatic Hydrocarbons in Biochar," Environ. Pollut., **171**, pp. 18–24.

[14] Buss, W., Graham, M. C., MacKinnon, G., and Mašek, O., 2016, "Strategies for Producing Biochars With Minimum PAH Contamination," J. Anal. Appl. Pyrolysis, **119**, pp. 24–30.

[15] Keiluweit, M., Kleber, M., Sparrow, M. A., Simoneit, B. R. T., and Prahl, F. G., 2012, "Solvent-Extractable Polycyclic Aromatic Hydrocarbons in Biochar: Influence of Pyrolysis Temperature and Feedstock," Environ. Sci. Technol., **46**(17), pp. 9333–9341.

[16] Wang, C., Wang, Y., and Herath, H. M. S. K., 2017, "Polycyclic Aromatic Hydrocarbons (PAHs) in Biochar—Their Formation, Occurrence and Analysis: A Review," Org. Geochem., **114**, pp. 1–11.

[17] Wilèn, C., Jukola, P., Järvinen, T., Sipilä, K., Verhoeff, F., and Kiel, J., 2013, "Wood Torrefaction—Pilot Tests and Utilisation," VTT Technol., **122**, pp. 1–80.

[18] Nanou, P., Carbo, M., and Kiel, J., 2015, "Biomass Torrefaction on Pilot Scale," Energy Research Centre of The Netherlands, Report No. ECN-M–15-034.

[19] Akinyemi, O. S., Jiang, L., Buchireddy, P. R., Barskov, S. O., Guillory, J. L., and Holmes, W., 2018, "Investigation of Effect of Biomass Torrefaction Temperature on Volatile Energy Recovery Through Combustion," ASME J. Energy Resour. Technol., **140**, pp. 1–11.

[20] Pawlak-Kruczek, H., Wnukowski, M., Krochmalny, K., Kowal, M., Baranowski, M., Zgóra, J., Czerep, M., Ostrycharczyk, M., and Niedzwiecki, L., 2019, "The Staged Thermal Conversion of Sewage Sludge in the Presence of Oxygen," ASME J. Energy Resour. Technol., **141**(7), p. 070701.

[21] M. Cremers, J. Koppejan, J. Middelkamp, J. Witkamp, S. Sokhansanj, S. Melin, and S. Madrali, 2015, "Status Overview of Torrefaction Technologies," IEA Bioenergy.

[22] Batidzirai, B., Mignot, A. P. R., Schakel, W. B., Junginger, H. M., and Faaij, A. P. C., 2013, "Biomass Torrefaction Technology: Techno-Economic Status and Future Prospects," Energy, **62**, pp. 196–214.

[23] González Martínez, M., Dupont, C., Thiéry, S., Meyer, X. M., and Gourdon, C., 2018, "Impact of Biomass Diversity on Torrefaction: Study of Solid Conversion and Volatile Species Formation Through an Innovative TGA-GC/MS Apparatus," Biomass Bioenergy, **119**, pp. 43–53.

[24] Lê Thành, K., Commandré, J.-M., Valette, J., Volle, G., and Meyer, M., 2015, "Detailed Identification and Quantification of the Condensable Species Released During Torrefaction of Lignocellulosic Biomasses," Fuel Process. Technol., **139**, pp. 226–235.

[25] Fagernäs, L., Kuoppala, E., and Arpiainen, V., 2015, "Composition, Utilization and Economic Assessment of Torrefaction Condensates," Energy Fuels, **29**(5), pp. 3134–3142.

[26] "Production of solid sustainable energy carriers from biomass by means of torrefaction (SECTOR)—Project Final Report Publishable," 2012, https://cordis.europa.eu/docs/results/282/282826/final1-sector_fpsr_rev_final.pdf

[27] Doddapaneni, T. R. K. C., Praveenkumar, R., Tolvanen, H., Palmroth, M. R. T., Konttinen, J., and Rintala, J., 2017, "Anaerobic Batch Conversion of Pine Wood Torrefaction Condensate," Bioresour. Technol., **225**, pp. 299–307.

[28] Jagodzińska, K., Czerep, M., Kudlek, E., Wnukowski, M., and Yang, W., 2019, "Torrefaction of Wheat-Barley Straw: Composition and Toxicity of Torrefaction Condensates," Biomass Bioenergy, **129**, p. 105335.

[29] Bergman, P. C. A., Boersma, A. R., Kiel, J. H. A., Prins, M. J., Ptasinski, K. J., and Janssen, F. J. J. G., 2005, "Torrefaction for Entrained-Flow Gasification of Biomass," Energy Research Centre of the Netherlands, Report No. ECN-RX—04-029, pp. 78–82.

[30] Tumuluru, J. S., Sokhansanj, S., Wright, C. T., and Kremer, T., 2012, "GC Analysis of Volatiles and Other Products From Biomass Torrefaction Process," Adv. Gas Chromatogr.: Prog. Agric., Biomed. Ind. Appl., pp. 211–234.

[31] Scott, R. P. W., 1998, *Introduction to Analytical Gas Chromatography*, Marcel Dekker, NY.

[32] Dhanavath, K. N., Bankupalli, S., Bhargava, S. K., and Parthasarathy, R., 2018, "An Experimental Study to Investigate the Effect of Torrefaction Temperature on the Kinetics of Gas Generation," J. Environ. Chem. Eng., **6**(2), pp. 3332–3341.

[33] Bach, Q. V., Chen, W. H., Chu, Y. S., and Skreiberg, Ø, 2016, "Predictions of Biochar Yield and Elemental Composition During Torrefaction of Forest Residues," Bioresour. Technol., **215**, pp. 239–246.

[34] Devi, P., and Saroha, A. K., 2015, "Effect of Pyrolysis Temperature on Polycyclic Aromatic Hydrocarbons Toxicity and Sorption Behaviour of Biochars Prepared by Pyrolysis of Paper Mill Effluent Treatment Plant Sludge," Bioresour. Technol., **192**, pp. 312–320.

[35] Weidemann, E., Buss, W., Edo, M., Mašek, O., and Jansson, S., 2017, "Correction to: Influence of Pyrolysis Temperature and Production Unit on Formation of Selected PAHs, oxy-PAHs, N-PACs, PCDDs, and PCDFs in Biochar—a Screening Study," Environ. Sci. Pollut. Res., **25**(4), pp. 3941–3942.

[36] Sun, M., Yang, Y., and Zhang, M., 2019, "A Temperature Model for Synchronized Ultrasonic Torrefaction and Pelleting of Biomass for Bioenergy Production," ASME J. Energy Resour. Technol., **141**(10), p. 102205.

[37] Stelte, W., Clemons, C., Holm, J. K., Sanadi, A. R., Ahrenfeldt, J., Shang, L., and Henriksen, U. B., 2011, "Pelletizing Properties of Torrefied Spruce," Biomass Bioenergy, **35**(11), pp. 4690–4698.

[38] EBC, 2016, "European Biochar Certificate—Guidelines for a Sustainable Production of Biochar," 10.13140/RG.2.1.4658.7043.

[39] Stelte, W., 2012, "Torrefaction of Unutilized Biomass Resources and Characterization of Torrefaction Gasses," http://www.teknologisk.dk/_root/media/52684_RK%20report%20torrefaction%20and%20torrefaction%20gas.pdf

[40] Chen, D., Gao, A., Ma, Z., Fei, D., Chang, Y., and Shen, C., 2018, "In-depth Study of Rice Husk Torrefaction: Characterization of Solid, Liquid and Gaseous Products, Oxygen Migration and Energy Yield," Bioresour. Technol., **253**, pp. 148–153.

[41] Nam, H., and Capareda, S., 2015, "Experimental Investigation of Torrefaction of Two Agricultural Wastes of Different Composition Using RSM (Response Surface Methodology)," Energy, **91**, pp. 507–516.

[42] Chen, D., Gao, A., Cen, K., Zhang, J., Cao, X., and Ma, Z., 2018, "Investigation of Biomass Torrefaction Based on Three Major Components: Hemicellulose, Cellulose, and Lignin," Energy Convers. Manag., **169**, pp. 228–237.

[43] Chen, W. H., Peng, J., and Bi, X. T., 2015, "A State-of-the-art Review of Biomass Torrefaction, Densification and Applications," Renew. Sustain. Energy Rev., **44**, pp. 847–866.

[44] Zheng, A., Jiang, L., Zhao, Z., Huang, Z., Zhao, K., Wei, G., Wang, X., He, F., and Li, H., 2015, "Impact of Torrefaction on the Chemical Structure and Catalytic Fast Pyrolysis Behavior of Hemicellulose, Lignin, and Cellulose," Energy Fuels, **29**(12), pp. 8027–8034.

[45] Grateau, M., Thiery, S., Salvador, S., Dupont, C., Nocquet, T., and Commandre, J. M., 2014, "Volatile Species Release During Torrefaction of Wood and its Macromolecular Constituents: Part 1—Experimental Study," Energy, **72**, pp. 180–187.

[46] Anca-Couce, A., Mehrabian, R., Scharler, R., and Obernberger, I., 2014, "Kinetic Scheme to Predict Product Composition of Biomass Torrefaction," Chem. Eng. Trans., **37**, pp. 43–48.

[47] Commandre, J. M., and Leboeuf, A., 2014, "Volatile Yields and Solid Grindability After Torrefaction of Various Biomass Types," Environ. Prog. Sustain. Energy, **34**(4), pp. 1180–1186.

[48] Werner, K., Pommer, L., and Broström, M., 2014, "Thermal Decomposition of Hemicelluloses," J. Anal. Appl. Pyrolysis, **110**, pp. 130–137.

[49] Martínez, M. G., Dupont, C., Meyer, X. M., and Gourdon, C., 2017, "Woody and Agricultural Biomass Diversity in Torrefaction: A Complete Study in Solid Conversion and Volatiles Formation on TGA-GCMS," Biochar: Production, Characterization and Applications, Alba, Italy, Aug. 20–25, pp. 1–20.

[50] Werle, S., and Dudziak, M., 2015, "The Assessment of Sewage Sludge Gasification by-Products Toxicity by Ecotoxicologial Test," Waste Manag. Res., **33**(8), pp. 696–703.

[51] Levén, L., Nyberg, K., Korkea-aho, L., and Schnürer, A., 2006, "Phenols in Anaerobic Digestion Processes and Inhibition of Ammonia Oxidising Bacteria (AOB) in Soil," Sci. Total Environ., **364**(1–3), pp. 229–238.

[52] Doddapaneni, T. R. K. C., Jain, R., Praveenkumar, R., Rintala, J., Romar, H., and Konttinen, J., 2018, "Adsorption of Furfural From Torrefaction Condensate Using Torrefied Biomass," Chem. Eng. J., **334**, pp. 558–568.

[53] Doddapaneni, T. R. K. C., Praveenkumar, R., Tolvanen, H., Rintala, J., and Konttinen, J., 2018, "Techno-Economic Evaluation of Integrating Torrefaction With Anaerobic Digestion," Appl. Energy, **213**, pp. 272–284.